2014-4

Microfiber Coupler Based Label-Free Immunosensor

Lin Bo
Technological University Dublin

Christy Charlton O'Mahony
Dublin City University

Yuliya Semenova
Technological University Dublin, yuliya.semenova@tudublin.ie

See next page for additional authors

Recommended Citation

O'Mahony, C. et al. (2014) Microfiber Coupler Based Label-Free Immunosensor. *Optics Express,* Vol.22, no.7,p.1169-1174. doi:10.1364/OE.22.008150

Funder: Enterprise Ireland under the international research grant MATERA ERA-NET

Microfiber coupler based label-free immunosensor

Lin Bo,[1,*] Christy Charlton O'Mahony,[2,3] Yuliya Semenova,[1] Niamh Gilmartin,[2] Pengfei Wang,[1,4] and Gerald Farrell[1]

[1]*Photonics Research Centre, Dublin Institute of Technology, Kevin Street, Dublin 8, Ireland*
[2]*Biomedical Diagnostics Institute, Dublin City University, Glasnevin, Dublin 9, Ireland*
[3]*School of Physical Sciences, Dublin City University, Glasnevin, Dublin 9, Ireland*
[4]*pengfei.wang@dit.ie*
[*]*D10122924@mydit.ie*

Abstract: Optical microfibers and related structures which incorporate large evanescent field and minimal size offer new opportunities for biosensing applications. In this paper we report the development of an immunosensor based on a tapered microfiber coupler embedded in a low refractive index polymer. Biomolecules adsorbed on the microfiber coupler surface modify the surrounding refractive index. By immobilizing antigens on the surface of the sensing area, the microfiber coupler was able to operate as a label-free immunosensor to detect specific antibodies. We experimentally demonstrated for the first time the sensing ability of this sensor using a fibrinogen antigen-antibody pair. By monitoring the spectral shift in the wavelength domain, the sensor was shown to be capable of detecting the specific binding between fibrinogen and anti-fibrinogen. The detected signal was found to be proportional to the anti-fibrinogen present.

OCIS codes: (060.2370) Fiber optics sensors; (280.1415) Biological sensing and sensors.

References and links

1. D. R. Thévenot, K. Toth, R. A. Durst, and G. S. Wilson, "Electrochemical biosensors: recommended definitions and classification," Biosens. Bioelectron. **16**(1-2), 121–131 (2001).
2. B. J. Tromberg, M. J. Sepaniak, T. Vo-Dinh, and G. D. Griffin, "Fiber-optic chemical sensors for competitive binding fluoroimmunoassay," Anal. Chem. **59**(8), 1226–1230 (1987).
3. G. P. Anderson and N. L. Nerurkar, "Improved fluoroimmunoassays using the dye Alexa Fluor 647 with the RAPTOR, a fiber optic biosensor," J. Immunol. Methods **271**(1-2), 17–24 (2002).
4. T. Endo, S. Yamamura, N. Nagatani, Y. Morita, Y. Takamura, and E. Tamiya, "Localized surface plasmon resonance based optical biosensor using surface modified nanoparticle layer for label-free monitoring of antigen–antibody reaction," Sci. Technol. Adv. Mater. **6**(5), 491–500 (2005).
5. J. M. Corres, J. Bravo, I. R. Matias, and F. J. Arregui, "Tapered optical fiber biosensor for the detection of anti-gliadin antibodies," Sens. Actuat. Biol. Chem. **135**, 166–171 (2008).
6. Y. Tian, W. Wang, N. Wu, X. Zou, and X. Wang, "Tapered optical fiber sensor for label-free detection of biomolecules," Sensors (Basel) **11**(12), 3780–3790 (2011).
7. L. Tong, R. R. Gattass, J. B. Ashcom, S. L. He, J. Y. Lou, M. Y. Shen, I. Maxwell, and E. Mazur, "Subwavelength-diameter silica wires for low-loss optical wave guiding," Nature **426**(6968), 816–819 (2003).
8. F. Xu, P. Horak, and G. Brambilla, "Optical microfiber coil resonator refractometric sensor," Opt. Express **15**(12), 7888–7893 (2007).
9. Y. Jung, G. Brambilla, and D. J. Richardson, "Optical microfiber coupler for broadband single-mode operation," Opt. Express **17**(7), 5273–5278 (2009).
10. P. Wang, M. Ding, G. Brambilla, Y. Semenova, Q. Wu, and G. Farrell, "High temperature performance of an optical microfiber coupler and its potential use as a sensor," Electron. Lett. **48**(5), 283–284 (2012).
11. L. Bo, P. Wang, Y. Semenova, and G. Farrell, "High sensitivity fiber refractometer based on an optical microfiber coupler," IEEE Photon. Technol. Lett. **25**(3), 228–230 (2013).
12. J. Vörös, "The density and refractive index of adsorbing protein layers," Biophys. J. **87**(1), 553–561 (2004).
13. H. Tazawa, T. Kanie, and M. Katayama, "Fiber-optic coupler sensors for biosensing," SEI Technical Review **65**, 67–70 (2007).
14. K. Okamoto, *Fundamentals of Optical Waveguides* (Elsevier Academic Press, 2006).

#194410 - $15.00 USD Received 31 Oct 2013; revised 1 Nov 2013; accepted 27 Nov 2013; published 1 Apr 2014

15. F. P. Payne, S. D. Hussey, and M. S. Yataki, "Polarisation analysis of strongly fused and weakly fused tapered couplers," Electron. Lett. **21**(13), 561–563 (1985).
16. G. Brambilla, V. Finazzi, and D. Richardson, "Ultra-low-loss optical fiber nanotapers," Opt. Express **12**(10), 2258–2263 (2004).
17. R. G. Lamont, D. C. Johnson, and K. O. Hill, "Power transfer in fused biconical-taper single-mode fiber couplers: dependence on external refractive index," Appl. Opt. **24**(3), 327–332 (1985).
18. F. Xu and G. Brambilla, "Embedding optical microfiber coil resonators in Teflon," Opt. Lett. **32**(15), 2164–2166 (2007).
19. G. Vienne, Y. Li, and L. Tong, "Effect of host polymer on microfiber resonator," IEEE Photon. Technol. Lett. **19**(18), 1386–1388 (2007).
20. Y. Semenova, L. Bo, P. Wang, S. Mathews, Q. Wu, M. Teng, C. Yu, and G. Farrell, "Experimental study of temperature response of a microfiber coupler sensor with a liquid crystal overlay," Proc., Fifth European Workshop on Optical Fibre Sensors (2013).

1. Introduction

A biosensor is an integrated receptor-transducer device, which is capable of providing selective quantitative or semi-quantitative analytical information using a biological recognition element [1]. The target analytes could be various bioparticles such as DNA, proteins, bacteria, etc. Among the variety of existing biosensors, biosensors which utilize antibodies as the recognition elements to detect specific antigens are categorized as immunosensors. Due to the high selectivity and sensitivity nature of antibodies for their antigen, immunosensors are in great demand for applications in clinical diagnosis, process control and environmental monitoring.

Given the well-known advantages of optical fiber based sensors, such as compact size, high resolution, immunity to electromagnetic interference and the potential for remote operation, several fiber optic immunosensors have been developed previously [2–4]. However, the majority of the proposed sensors require the use of a label which significantly increases complexity. Several label-free immunosensors have been recently demonstrated which consist of simple structures based on nonadiabatic tapered optical fibers [5, 6]. Such sensors utilize the evanescent field of the tapered fiber region to enhance the light-biomaterial interaction for biosensing applications.

Silica subwavelength diameter optical fibers have attracted the interest of researchers since Tong's first demonstration in 2003 [7]. Microfibers have unique properties such as a very large evanescent field, strong mode confinement and micro-scale diameters. As a result, subwavelength diameter optical fibers or simply "microfibers" offer opportunities for new biosensing techniques [8]. In particular, microfibers and related structures have the potential to achieve label-free detection with an even higher sensitivity and a faster response, but with a compact size significantly smaller than macro-sized fiber tapers. Following the demonstration and application of a single-mode microfiber coupler (MFC) [9, 10], we presented a high sensitivity refractometer based on an MFC structure in [11]. The refractometer achieved an average sensitivity of 2723 nm/RIU and a maximum sensitivity of over 4000 nm/RIU in the refractive index (RI) range from 1.334 to 1.38. Given that the surrounding RI is usually modified by biomolecules adsorbed on the fiber surface [12], the MFC has the potential to work as a biosensor. A biosensor based on a conventional fused fiber coupler was proposed by Tazawa et al. in 2007 [13]. The authors showed the ability of the coupler to be used for protein detection using an avidin-biotin interaction. In this paper, for the first time we experimentally demonstrate an immunosensor based on an MFC structure. The sensor is capable of detecting the specific binding between fibrinogen and anti-fibrinogen.

2. Principle of operation

An MFC has the same structure as a conventional fused fiber coupler, except for a much smaller waist diameter (approximate 1-2 μm) [9]. The MFC is fabricated by tapering and laterally fusing two single-mode fibers together at the same time. As the fibers are being tapered and fused, the light starts to interchange between the two adjacent fibers. This light

#194410 - $15.00 USD Received 31 Oct 2013; revised 1 Nov 2013; accepted 27 Nov 2013; published 1 Apr 2014

interchange is due to the difference in the propagation constants between the even and odd modes [14] or symmetric and anti-symmetric modes as presented in some literatures [15]. As the diameter of the fiber coupler reduces, the fiber coupler reaches a state where it displays a strong evanescent field and where the transmission spectrum shows a semi-periodically resonant behavior for each of the output ports. The former is due to the wavelength-scale waist diameter of the tapered fibers. The latter is due to the even-odd mode interference between the fused fibers. With these light transmission properties, such an MFC has strong potential to work as a wavelength-domain sensor with good sensitivity.

We have previously shown that a change in the surrounding RI will strongly influence the MFC transmission spectrum [11]. This points to a possible approach to implement an immunosensor using such an MFC. The antibodies adhere to the MFC surface due to physical adsorption which in turn allows the binding of the corresponding antigen. When the specific binding between the antibody and the antigen occurs, the surface RI of the MFC is increased and thus detectable peak wavelength shifts over the transmission spectra occur. In this experiment, we used a fibrinogen antigen-antibody pair as the biosensing elements to evaluate the immunosensing performance of the embedded MFC. Fibrinogen has excellent immobilizing properties on silica surfaces. As a result, the need for MFC surface treatment to promote adherence is avoided with fibrinogen immobilization. For this reason, we used fibrinogen (antigen) as the receptor and anti-fibrinogen (antibody) as the analyte to demonstrate the principle and operation of the proposed immunosensor in this work.

3. Sensor fabrication

3.1 MFC fabrication

An MFC was fabricated by fusing and tapering two single-mode optical fibers together using the microheater brushing technique demonstrated in [16]. The fabricated MFC had a 3 mm long uniform waist region and two 13 mm long transition regions on each side. The MFC was weakly fused and the minimum tapered diameter of each fiber was approximately 2 μm. The weakly fused condition is important because when the coupler is weakly fused, the coupling coefficient has a stronger dependence on the surrounding RI change [17].

3.2 MFC embedding

A free standing MFC suffers from poor mechanical stability and therefore could be affected by environmental influences. The experimental processes can also disturb the MFC and result in large measurement errors. In order to achieve accurate sensing results, a stable sensing system is essential. We embedded the MFC in a low refractive index UV curable polymer (Efiron UVF PC363, Luvantix) to improve the system stability during measurements. The embedding technique was similar to that demonstrated in [18, 19] with modifications for sensing applications. A microscope slide was first covered with a thin layer of the UV curable polymer. Two blocks of polydimethylsiloxane (PDMS) were placed in parallel on the polymer surface to create an open-top channel. The fabricated microfiber coupler was placed into the channel in such a way that the bottom of the coupler was stuck to the polymer surface while the rest of the coupler was still exposed to the local environment. Then we placed several drops of the viscous UV curable Efiron polymer to block the two ends of the channel and also to fix the coupler in place. The 20 mm long section in the center was left uncovered as a sensing window for the biosensing experiments. Then the entire device was cured using UV radiation (CS2010 UV Curing LED System, Thorlabs) for 30 second. The refractive index of the cured polymer is approximately 1.36. During the biosensing experiment, the liquid analyte is placed in and removed from the channel using a pipette. The experimental setup is shown schematically in Fig. 1. Light from a broadband source (BBS) (Fiber Coupled SLD, Thorlabs) was injected into the input port. The output signal was detected with an optical spectrum analyzer (OSA) (86142B, Agilent).

#194410 - $15.00 USD Received 31 Oct 2013; revised 1 Nov 2013; accepted 27 Nov 2013; published 1 Apr 2014

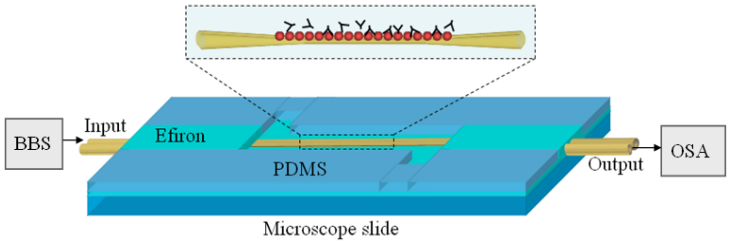

Fig. 1. Schematic diagram of the embedded MFC and the experimental setup.

3.3 Fibrinogen immobilization

Human fibrinogen (95% clottable and plasminogen depleted) was purchased from Calbiochem, Merck KGaA. Before immobilizing the fibrinogen, a baseline spectrum of the MFC was measured. For this the MFC sensing area was fully covered with 0.2 ml phosphate-buffered saline (PBS) and the transmission spectrum was recorded as the baseline. Then the PBS was removed and replaced with fibrinogen solution in PBS buffer (0.2 ml, 100 μg/ml). The solution was left to settle for 20 minutes so the fibrinogen molecules could fully adsorb to the exposed MFC fiber surface. In order to measure the change caused by the immobilized fibrinogen only, the sensing area was then rinsed with the PBS buffer several times. The rinse step returned the liquid environment to the baseline level and also removed any loosely bound fibrinogen. Figure 2(a) shows a typical example of the transmission spectrum evolution during the fibrinogen immobilization. The evolution in time of the fibrinogen immobilization profile is shown in Fig. 2 (b). A rapid shift occurs in the first 5 minutes, followed by a much slower shift. The shift reaches a plateau within 20 minutes which indicates that the MFC surface has been fully occupied by the fibrinogen molecules. A total blueshift of 13.6 nm was observed for the entire immobilization process.

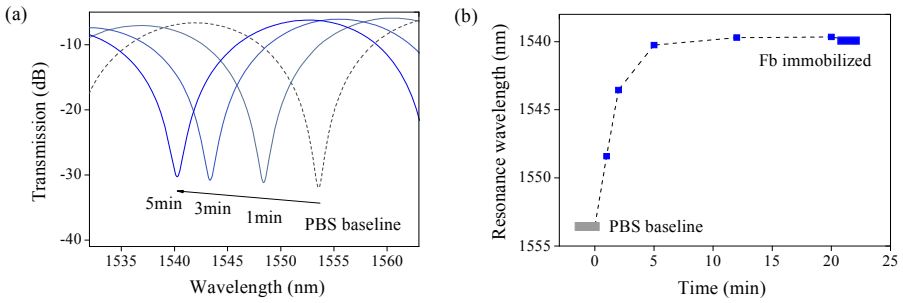

Fig. 2. (a). Spectral response during the first 5 min of the fibrinogen immobilization on the MFC surface; (b) Time-dependent profile of the fibrinogen immobilization.

For the 15 samples we studied, the fibrinogen immobilization caused an average blueshift of 12.22 nm with a standard deviation of 1.51 nm, as shown in the lower section of Fig. 3. We believe the discrepancy in the fibrinogen immobilization among the samples mainly results from the limited precision in the MFC fabrication. For example the tapered diameter and the coupling length for each MFC sample may vary. This is suggested by the variation in the free spectral range (FSR) among the samples, as shown in the upper section of Fig. 3.

#194410 - $15.00 USD Received 31 Oct 2013; revised 1 Nov 2013; accepted 27 Nov 2013; published 1 Apr 2014

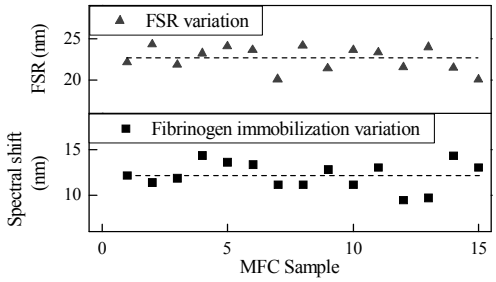

Fig. 3. Signal changes caused by the fibrinogen immobilization for the 15 studied MFC samples.

4. Biosensing experiment, results and discussion

We use fibrinogen as the recognition element to detect anti-fibrinogen, as mentioned previously. Once the fibrinogen was immobilized on the MFC surface, we applied rabbit anti-fibrinogen solution (Calbiochem, Merck, KGaA) in PBS buffer (0.2 ml, 100 µg/ml) to the sensor. The anti-fibrinogen solution was left to settle for 60 min and the measurement was taken after the rinse step. In order to verify the selectivity of the sensor for anti-fibrinogen among unspecific antibodies, a negative control was performed using Immunoglobulin G antibody (goat anti-human IgG, Sigma Aldrich). The control was performed with the same procedure above using an anti-IgG solution in PBS buffer (0.2 ml, 100 µg/ml).

Figure 4 illustrates the typical behavior of the sensor in distinguishing between the anti-fibrinogen and the anti-IgG. The binding between the anti-fibrinogen and the fibrinogen occurs gradually over a period of 60 minutes. The total blueshift caused by the bound layer of anti-fibrinogen molecules is 10.35 nm. The anti-IgG control causes a 0.45 nm redshift over the same length of time given that the fibrinogen does not specifically interact with the anti-IgG. The significant difference between the two shifts indicates that the sensor is capable of distinguishing between the specific anti-fibrinogen and the non-specific anti-IgG. The relatively small redshift caused by the anti-IgG is most likely a result of measurement error. The error can be caused by (1) temperature drift (the temperature dependence of an embedded MFC with similar parameters was given in [20]); (2) small mechanical displacement of the MFC during the application and removal of solutions; (3) desorption of a small amount of the loosely bound fibrinogen molecules from the MFC surface.

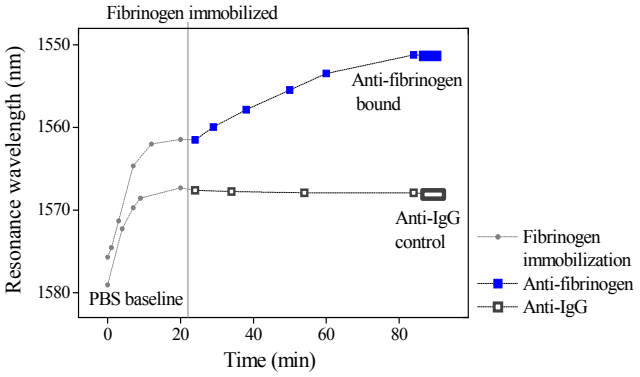

Fig. 4. Comparison of the sensor behavior for the anti-fibrinogen detection and for the anti-IgG control. The experiments were carried out on two individual sensors. A 10.35 nm blueshift was observed for the anti-fibrinogen detection while a 0.45 nm redshift was observed for the anti-IgG control.

#194410 - $15.00 USD Received 31 Oct 2013; revised 1 Nov 2013; accepted 27 Nov 2013; published 1 Apr 2014

We repeated the experiment using anti-fibrinogen solutions with various concentrations ranging from 25μg/ml to 100 μg/ml. The concentration of the fibrinogen solution remained constant at 100 μg/ml. The sensing results are shown in Fig. 5. One can see that the detected signal increases with the increasing concentration of the anti-fibrinogen solution. This indicates that the detected signal for the sensor is proportional to the amount of the anti-fibrinogen present. The results, as shown in the control data point in Fig. 5, are consistent and demonstrate the selectivity of the sensor between the positive and the negative analytes.

In order to gauge repeatability, the experiment was repeated three times for each concentration and furthermore each repetition was performed on a newly fabricated sensor. We also repeated the control experiment several times. The errors bars in Fig. 5. represent the standard deviation of the repeated measurement results at each concentration and confirm the good repeatability of the sensor. The most likely reason for the variations in the spectral shifts for the anti-fibrinogen sensing experiment are small physical differences among the MFC samples, as previously mentioned in relation to Fig. 3. Temperature fluctuations may also be a contributing factor. The mechanisms behind the protein adsorption and binding regimes are beyond the scope of this paper.

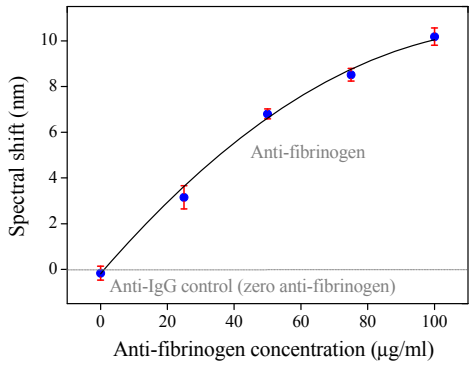

Fig. 5. Variations in the spectral shift caused by anti-fibrinogen with the fibrinogen solution concentrations (25 μg/ml, 50 μg/ml, 75 μg/ml and 100 μg/ml). The experiment was repeated 3 times for each concentration. All the repetitions were performed individually on newly fabricated sensors. The solid line is the polynomial fitting of the mean of the measurements.

5. Conclusions

A label-free immunosensor based on an embedded MFC has been experimentally demonstrated using a fibrinogen antigen-antibody pair. The sensor has been fabricated by immobilizing fibrinogen on the sensing surface of the embedded MFC. The performance of the sensor in identifying anti-fibrinogen in the wavelength domain has been evaluated. Results showed that the MFC based immunosensor is capable of detecting anti-fibrinogen and that the detected signal is proportional to the amount of the anti-fibrinogen present. Given the advantages such as label-free detection, fast response and easy fabrication, this MFC based biosensor offers a reliable, compact and simple solution in current immunoassay.

Acknowledgments

The authors wish to thank Claire Wynne of the DIT School of Biological Sciences for her advice and guidance. Lin Bo acknowledges support from the International Centre for Graduate Education in micro & nano Engineering (ICGEE) for her PhD funding. Pengfei Wang is funded by the Irish Research Council (IRC) and co-funded by the EU Marie-Curie Actions under FP7.